Organic Process Research & Development **2007**, *11*, 846–860

Characterization of the Polymorphic Behavior of an Organic Compound Using a Dynamic Thermal and X-ray Powder Diffraction Technique

David Albers,‡ Michelle Galgoci,† Dan King,‡ Daniel Miller,† Robert Newman,*,‡ Linda Peerey,‡ Eva Tai,† and Richard Wolf†

Dowpharma Department, The Dow Chemical Company, 1710 Building, and Department of Analytical Sciences, The Dow Chemical Company, 1897 Building, Midland, Michigan 48674, U.S.A.

Abstract:

The crystalline polymorphic forms of several samples of an organic compound produced by Dowpharma were characterized using differential scanning calorimetry (DSC); X-ray powder diffraction (XRPD); combined, simultaneous, and dynamic differential scanning calorimetry/X-ray powder diffraction (DSC/XRPD); and high performance liquid chromatography (HPLC). A total of 10 crystalline polymorphs were identified, six of which are anhydrous. Form I is a heptahydrate that reversibly converts to anhydrous Form I under dry conditions and also undergoes a reversible solid–solid phase transition at about 110 °C to convert to Form II. Form II is anhydrous and melts at approximately 220 °C. Form III crystallizes as a hexahydrate, which reversibly converts to the monohydrate Form III and then to an anhydrous Form III above 120 °C. Anhydrous Form III melts at approximately 200 °C. Form IV crystallized as a hydrous material, which was converted to the anhydrous Form IV above approximately 60 °C, in a reversible process. Form IV appears to be unstable in high humidity conditions (e.g., 90% relative humidity at 25 °C) and slowly converts to Forms I and III. Form IV also undergoes a nonreversible solid–solid phase transition at approximately 180 °C, to form anhydrous Form V. Form V melts at approximately 245 °C. Form VI is observed only in the anhydrous state and melts at approximately 245 °C. The anhydrous nature of Form VI makes this material the most ideal crystalline material for subsequent formulation work.

1. Introduction

The rational control of polymorphs of active pharmaceutical ingredients (API) has been an important goal for the pharmaceutical industry. Differential scanning calorimetry (DSC) and X-ray powder diffraction (XRPD) analyses of API solids have been important methods for determining polymorphism for several years. DSC is still used as a stand-alone tool for these determinations.[1,2] However, XRPD has become the gold standard method for API polymorphism determinations. Two recent reviews on the importance of XRPD in the pharmaceutical industry have been written.[3,4] Other multivariate methods for quality control of API polymorphism have been developed. These include diffuse reflectance Fourier transfer IR (DRIFT--IR),[5,6] focused beam reflectance measurement (FBRM),[7] and particle vision and measurement (PVM).[7] These latter methods depend, however, on XRPD as a reference and confirmation technique. Recent publications on the use of XRPD for API polymorphism analyses include the characterization of three polymorphic forms of acitretin,[8] the study of a stable polymorph of paclitaxel,[9] and the study of three polymorphs of sibenadet hydrochloride.[10]

DSC and XRPD have typically been used as separate techniques to study the polymorphism of the same compound, with XRPD as the confirming methodology. Thus, a combination of separately used DSC and XRPD has been used to study nifedipine (along with the use of FTIR),[11] bicifadine (along with the use of thermogravimetric analysis (TGA), attenuated total reflectance (ATR) IR and ATR-near-IR),[12] methotrexate (along with TGA),[13] carbamazepine (along with FTIR and hot-stage FTIR thermomicroscopy),[14] ranitidine hydrochloride,[15] terfenadine,[16] zanoterone (along with FTIR),[17] dehydroepiandrosterone (with IR)[18] and 3-[[[3-2[-(7-chloro-2-quinolinyl)-(*E*)-ethenyl]phenyl][[3-dimethylamino-3-oxopropyl]thio]methyl]thio]propanoic acid.[19] Increased use of variable temperature XRPD has been noted in the literature. Polymorphic solid state changes

---

* To whom correspondence should be addressed. Telephone: 989 636-4001. Fax: 989 638-9716 . E-mail: ra_newman@dow.com.

‡ Department of Analytical Sciences.

† Dowpharma Department.

(1) Park, K; Evans, J. M. B.; Myerson, A. S. *Cryst. Growth Des.* **2003**, *3*, 991–995.

(2) Hino, T.; Ford, J. L.; Powell, M. W. *Thermochimica Acta* **2001**, *374*, 85–92.

(3) Byrn, S. R.; Bates, S.; Ivanisevic, I. *Am. Pharm. Rev.* **2005**, *8*, 55–59.

(4) Litteer, B.; Beckers, D. *Am. Lab.* **2005**, *37*, 22–24.

(5) Poellaenen, K.; Haekkinen, A.; Huhtanen, M.; Reinkainen, S.-P.; Karjalainen, M.; Rantanen, J.; Louhi-Kultanen, M.; Nystoem, L. *Anal. Chim. Acta* **2005**, *544*, 108–117.

(6) Agatonovic-Kustrin, S.; Rades, T.; Wu, V.; Saville, D.; Tucker, I. G. *J. Pharm. Biomed. Anal.* **2001**, *25*, 741–750.

(7) O'Sullivan, B.; Barrett, P.; Hsiao, G.; Carr, A.; Glennon, B. *Org. Process Res. Dev.* **2003**, *7*, 977–982.

(8) Malpezzi, L.; Magnone, G. A.; Masciocchi, N.; Sironi, A. *J. Pharm. Sci.s* **2005**, *94*, 1067–1078.

(9) Harper, J. K.; Barich, D. H.; Heider, E. M.; Grant, D. M.; Franke, R. R.; Johnson, J. H.; Zhang, Y.; less, P. L.; Von Dreele, R. B.; Scott, B.; Williams, D.; Ansell, G. B. *Cryst. Growth Des.* **2005**, *5*, 1737–1742.

(10) Cosgrove, S. D.; Steele, G.; Austin, T. K.; Plumb, A. P.; Stensland, B.; Ferrari, E.; Roberts, K. J. *J. Pharm. Sci.* **2005**, *94*, 2403–2415.

(11) Song, M.; Liebenberg, W.; de Villiers, M. M. *Pharmazie* **2006**, *61*, 336–340.

(12) McArdle, P.; Gilligan, K.; Cunningham, D.; Ryder, A. *Appl. Spectrosc.* **2005**, *59*, 1365–1371.

(13) Nikander, H; Tittanen, S. *Res. Disclosure* **2004**, *486*, 1252–1254.

(14) Rustichelli, C.; Gamberini, G.; Ferioli, V.; Gamberini, M. C.; Ficarra, R.; Tommasini, S. *J. Pharm. Biomed. Anal.* **2000**, *23*, 41–54.

(15) Wu, V.; Rades, T.; Saville, D. J. *Pharmazie* **2000**, *55*, 508–512.

(16) Sheikh, S. M.; Pillai, G. K.; Nabulsi, L.; Al-Kaysi, H. N.; Arafat, T. A.; Malooh, A. A.; Saleh, M.; Badwan, A. A. *Int. J. Pharm.* **1996**, *141*, 257–259.

(17) Rocco, W. L.; Morphet, C.; Laughlin, S. M. *Int. J. Pharm.* **1995**, *122*, 17–25.

(18) Chang, L.-C.; Caira, M. R.; Guillory, J. K. *J. Pharm. Sci.* **1995**, *84*, 1169–1179.

(19) Ghodbane, S.; McCauley, J. A. *Int. J. Pharm.* **1990**, *59*, 281–286.

10.1021/op700037w CCC: $37.00

Table 1. **Summary of methods of preparation of samples for combined DSC/XRD**

sample no.	form	description of preparation[a]
8	I and IV	sample 38 and 95/5 acetone/water held at 52 °C for 2 h
9	I + ?	sample 11, redissolved into 50/50 acetone/water, then Step 1[b]; wetcake slurried with 95/5 acetone/water at 52 °C for 4 h, isolated cold solids and dried at 73 °C/25 h
10	I	95/5 acetone/water mother liquor from sample 9, after evaporation to leave solids
11	I	Step 1, but kept 50/50 acetone/water solution at 49 °C and seeded with Form III; solids at 47.5 °C, cooled to 5 °C and isolated solids
26	amorphous	lyophilized aqueous solution of **1** disodium salt
33	I	Step 1, then slurried wetcake in 95/5 acetone/water up to 54 °C for 3.2 h, then isolated solids and dried at 69 °C for 15 h
34	I	Step 1, then dried solids at 50 °C/1.7 h
35	III	sample 34, heated to reflux as 95/5 acetone/water slurry for 1.5 h; isolated solids and dried at 42 °C/4 h
38	I	Step 1 with precipitation at 37 °C, and solids dried at 40 °C/3 h
40	VI	sample 38 refluxed with anhydrous acetone (acetone/solids 13.1/1 v/w) for 3.2 h as slurry, then solids isolated and dried in air
45	I + III	Step 1, but all processes done in 70/30 acetone/water, with heating to 50 °C to dissolve solids; isolated and dried solids at 38 °C/15 h
49	III hydrate	Step 1, then heated wetcake in 95/5 acetone/water to reflux for 1.3 h, then isolated solids and dried at 48 °C for 15 h
50	I	Step 1, then slurried wetcake in 95/5 acetone/water up to 52 °C for 2.4 h, then isolated solids and dried at 50 °C for 3 h
56	III + IV	heated sample 49 to reflux as slurry in 95/5 acetone/water for 2 h; a very thick “milkshake” mixture set up; solids were isolated, washed with acetone, and allowed to dry in air
57	IV hydrate	sample 50 was refluxed as slurry in 95/5 acetone/water, isolated solids at 5 °C and allowed to dry in air
59	I + III + IV + (VI?)	sample 50, held in 95/5 acetone/water at 50 °C for 1 h; mixture IV + (VI?) set up to make “milkshake” slurry; solids isolated at 5 °C and allowed to dry in air
62	V anhydrous	sample 57 was heated to 200 °C in a helium atmosphere and then allowed to cool to ambient temperature

[a] All drying under vacuum, except as noted. The Step 2 preparation of Form I hydrate involved either stirring the Step 1 wetcake in 95/5 (v/v) acetone/water at ambient temperature for more than 10 h or heating the Step 1 wetcake in 95/5 acetone/water below the reflux temperature for more than 1.5 h. [b] The Step 1 preparation of **1** dicarboxylate disodium salt involved complete dissolution of **1** dicarboxylic acid into a 50/50 acetone/water (v/v) solution at a temperature of 46–48 °C with a 3–6% excess of sodium bicarbonate to produce the disodium salt. Acetone was then added to make a 70/30 acetone/water solution. The solution was cooled to precipitate and isolate the solids as a wetcake.

using this technique have been reported for sulfathiazole, theophylline, and nitrofurantoin.[20,21] The variable temperature XRPD technique has been reviewed recently.[22,23] The present manuscript reports the use of a unique Dow-developed combined DSC/XRPD instrument[24–26] to dynamically characterize the polymorphic behavior of an organic compound API over a temperature range of hundreds of degrees. This allows the simultaneous measurements of thermochemical and thermophysical events, while following changes in crystalline structure (polymorphism) during these events.

2. Results and Discussion

The compound (**1**) of this study was a disodium salt of an organic dicarboxylic acid of molecular weight of about 400. Representative sample preparation conditions of various forms of **1** are given in Table 1. Note that a common starting material for the preparation of these samples was the wetcake from Step 1. The Step 1 preparation of **1** disodium salt involved complete dissolution of **1** dicarboxylic acid into a 50/50 (v/v) acetone/water solution at a temperature of 46–48 °C with a 3–6% excess of sodium bicarbonate to produce the disodium salt. Acetone was then added to make a 70/30 acetone/water solution. The solution was cooled to precipitate and isolate the solids as a wetcake. In the following discussions, generalizations on the conditions found to produce the various crystalline forms of **1** disodium salt are noted, along with discussions on the thermal and XRPD characterization of each form. The ability to simultaneously observe dynamic thermal events (via DSC) and the corresponding structural events (via XRPD) through use of the DSC/XRPD instrument (Figure 1) greatly accelerated

---

(20) Karjalainen, M.; Airaksinen, S.; Rantenen, J.; Aaltonen, J.; Yiruusi, J. *J. Pharm. Biomed. Anal.* **2005**, *39*, 27–32.

(21) Airaksinen, S.; Karjalainen, M.; Raessaenen, E.; Rantanen, J.; Yiruusi, J. *Int. J. Pharm.* **2004**, *276*, 129–141.

(22) Brittain, H. G. *Am. Pharm. Rev.* **2002**, *5*, 74–76.

(23) Brittain, H. G. *Spectroscopy* **2001**, *16*, 14–16–18.

(24) Fawcett, T. G.; Martin, E. J.; Crowder, C. E.; Kincaid, P. J.; Strandjord, A. J.; Blazy, J. A.; Armentrout, D. N.; Newman, R. A. *Adv. X-Ray Anal.* **1986**, *29*, 323–332.

(25) Fawcett, T. G.; et al. *Chemtech* **1987**, 564–569.

(26) Fawcett, T. G.; Harris, W. C., Jr. Newman, R. A.; Whiting, L. F.; Knoll, F. J. U. S. Patent 4,821,303, 1989.

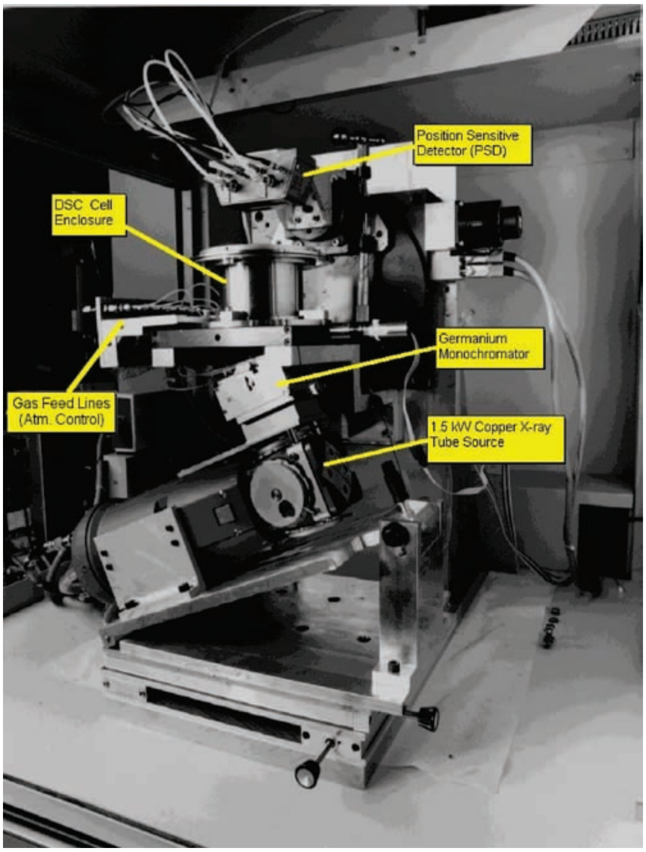

Figure 1. **Second generation Dow-developed DSC/XRPD instrument. Disruption of the thermal environment of the DSC was minimized by creating a ~1 mm diameter vertical X-ray beam path through the center of the sample and reference sensors of the DSC cell. Thermal isolation was maintained by using beryllium metal foil to seal the X-ray optical path.**

identification and understanding of the thermal behavior of the various polymorphic forms found.

It should be noted that throughout this paper there are references to samples with disparate numbering. This is due to the fact that, in a complex multi-polymorph system (such as this), one often re-creates "old" polymorphs during the process of developing control of the system to produce the desired form for development and testing.

DSC data, suggested forms, and additional characterizations of representative samples of pure polymorphs of **1** are given in Table 2. Combined DSC/XRPD data, suggested forms, and additional characterizations of representative samples of pure polymorphs of **1** are given in Table 3. Combined DSC/XRPD data, suggested forms, and additional characterizations of representative samples of polymorph mixtures of **1** are given in Table 4.

Forms I and II.

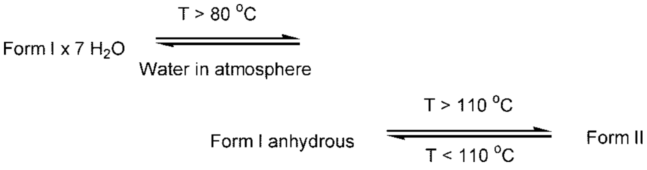

Form I has been typically produced during a purification re-slurry of material from Step 1 in a 95/5 (v/v) acetone/water solution between 48 and 54 °C for several hours while being careful to avoid refluxing the sample. This re-slurry process is referred to as Step 2 and has typically produced Form I. The heptahydrate Form I is uniquely identified by DSC analyses, by the presence of a large single endotherm below 80 °C and by a small (4–8 J/g) reversible solid–solid phase transition that occurs with an onset between 100 and 110 °C. Above 110 °C, a new crystalline form, Form II, is produced. Form II melts with an onset of approximately 210–215 °C, with an apparent heat of fusion of 30–45 J/gram. Typical DSC results attributed to Form I are shown in Figures 2 (hydrate) and 3 (anhydrous), and numerical results for representative examples are tabulated in Table 2. The relatively large variation in the heat of fusion may be due to two factors. First, the integration is difficult because an exotherm due to sample degradation immediately follows the melt and creates an uncertain baseline. Second, the varying quantities of water in the starting material (Form I) result

Table 2. **Summary of DSC data, suggested results, and additional characterizations**

sample no.	peak onsets (°C)	peak max (°C)	peak area (J/g)	suggested form	thermal event[a]
3[b]	19	92	76	III monohydrate	loss of water
	178	186	41		melt of Form III?
4	76	107	81	III monohydrate	loss of water
	190	201	37		melt of Form III
5	107	111	9	I	Form I to Form II
	207	222	47		melt of Form II
7	99	117	83	III monohydrate	loss of water
	189	202	44		melt of Form III
9	110	113	8	I	Form I to Form II
	213	226	54		melt of Form II
12	106	111	9	I	Form I to Form II
	213	226	56		melt of Form II
17[b,c]	238	249	52	VI	melt of Form VI
21[c]	242	252	68	VI	melt of Form VI
22	104	109	5	I	Form I to Form II
	210	224	30		melt of Form II
24	2	36	9	VI hydrate	loss of water
	255	266	41		melt of Form VI
25[b]	2	22	3	VI hydrate	loss of water
	258	266	63		melt of Form VI

[a] Endotherms. [b] XRPD data obtained separately. [c] Light microscopy also performed on sample.

Table 3. **Summary of combined DSC/XRD data, suggested results, and additional characterizations**

sample no.	peak onsets (°C)	peak max (°C)	peak area (J/g)	suggested form	thermal event	figures[a]
11	98	103	2	I	Form I to Form II	
	203	213	38		melt of Form II	
46	110	113	8	I	Form I to Form II	5
	213	225	40		melt of Form II	4
10	26	60	301	I hydrate	loss of water	
	188	205	15	I	melt of Form I	
33	106	110	7	I	Form I to Form II	3, 23
	211	225	45		melt of Form II	3
35	5	47-74-113	110 (total)	III hydrate	loss of water	10, 14
	196	206	37		melt of Form III	10
40	249	257	46	VI	melt of Form VI	22, 23
26	1	50	141	amorphous	loss of water	24, 25
	156	164	2		melt of amorphous	24
49	12	45	320	III hydrate	loss of water	11, 12, 13, 14
57	21	59	98	IV hydrate	loss of water	16, 17, 18, 23
	177	183	9		Form IV to Form V	17, 18
	245	256	34		melt of Form V	17
62	246	257	46	V anhydrous	melt of form V	18, 19

[a] Only selected figures have been included in report to illustrate behavior of the different polymorphs.

Table 4. **Mixtures of polymorphs in selected samples as analyzed by DSC and XRPD**

sample number	peak onsets (°C)	peak max (°C)	peak area (J/g)	suggested form[a]	thermal event[b]	figures[c]
2	<20	57	38	I and III hydrates	loss of water	
	187	200	45		melt of Forms I and III	
8[e]	22	50	50	I and IV hydrates	loss of water	30
	108	110	1		Form I to Form II	30
	181	187	9		Form IV to Form V	30
	215	224	4		melt of Form II	30
	246	255	30		melt of Form V	30
13	−2	45	24	VI + (IV or III monohydrate)	loss of water	
	174	181	2		Form IV to Form V?	
	231	248	36		melt of Form VI + III, V	
14	10	53	38	VI + (IV or III monohydrate)	loss of water	
	174	179	2		Form IV to Form V?	
	231	248	36		melt Form VI + III, V	
20[d]	190	198	1	VI + (III)	melt of Form III	
	239	250	57		melt of Form VI	
45	22	52	225	hydrated I and III	loss of water	26
	100	111	8		Form I to Form II	26
	194	205	16		melt of Form III	26
	205	218	12		melt of Form II	26
52	26	55	313	hydrated I + “New”	loss of water	34, 35
	99	103	5	“New” form	Form I to Form II	34
	159	166			unknown	34
	188	202	9		melt of atypical Form II	34
56[e]	14	56	116	III monohydrate + IV hydrate	loss of water	31, 32
	171	185	4		Form IV to Form V	31
	190	201	20		melt of Form III	31
	242	252	9		melt of Form V	31
58[e]		113		anhydrous I + III monohydrate	Form I to Form II	28, 29
	132	138	1		loss of water (III)	28, 29
	186	200	13		melt of Form III	28
	209	221	22		melt of Form II	28
59[e]	13	53	74	I + III + IV + (VI?)	loss of water	33
	<100	118	2		Form I to Form II	33
	167	182	2		Form IV to Form V	33
	188	201			melt of Form III,	33
		222			melt of Form II,	33
		252	41(total)		melt of Form V (and VI?)	33
60	111	113	5	I + III	Form I to Form II	27
	195	205	14		melt of Form III	27
	215	228	27		melt of Form II	27

[a] Forms identified in parentheses appear to be more minor components, present in small quantities. [b] Endotherms. [c] Only selected figures have been included in report to illustrate behavior of the different polymorphs. [d] XRPD obtained separately. [e] XRPD obtained concurrently with DSC using DSC/XRPD instrument.

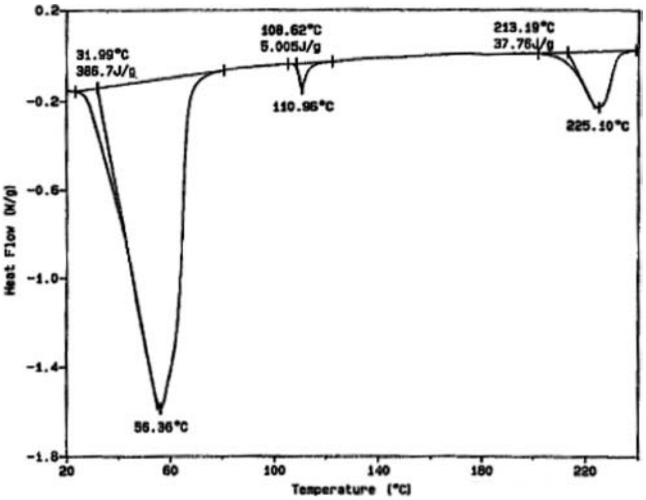

Figure 2. **DSC of hydrated Form I (sample 31).**

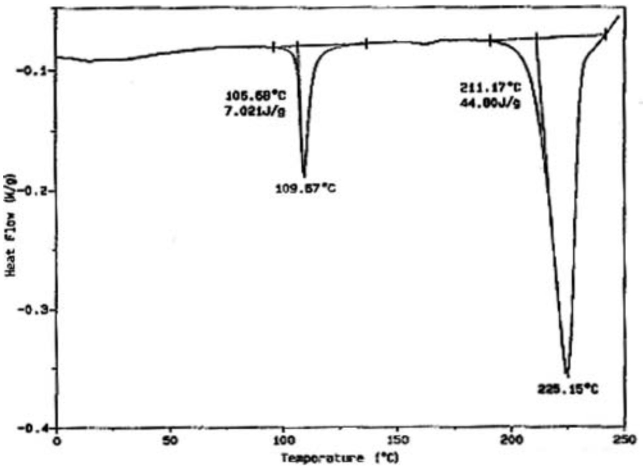

Figure 3. **DSC of anhydrous Form I (sample 33).**

in up to a 14% weight loss, due to water evolution. Corrections due to varying water content have not been made in these data.

Two experiments were performed to identify the 110 °C endotherm as a reversible solid–solid state phase transition. In the first experiment, three consecutive DSC trials were performed, wherein the sample was first heated to approximately 160 °C, then cooled down to approximately 45 °C, re-scanned to approximately 225 °C, cooled down again, and subsequently scanned to 240 °C. The results are shown in Figure 4. The solid–solid phase transition endotherm was observed again during the first re-scan but at a slightly lower onset temperature of 100 °C. Evolved gas analysis using thermal gravimetric/mass spectrometry (TG/MS) indicated that trace quantities of acetone were evolved above 120 °C. Different purities between the first and second scan may have contributed to the small shift in the onset temperature. The endotherm was not observed during the third scan, because the sample melted at 210 °C during the second scan. In the third scan, only a small peak at approximately 170 °C was observed. The second experiment involved DSC/XRPD analyses, and the results are shown in Figure 5. At 110 °C, the powder diffraction pattern began to change, indicating the structural conversion to Form II. As the sample was cooled, the diffraction pattern began to revert back to the XRPD pattern for anhydrous Form I at 100 °C. These results verified that the 110 °C endotherm is a reversible solid–solid structural phase transition between anhydrous Form I and anhydrous Form II.

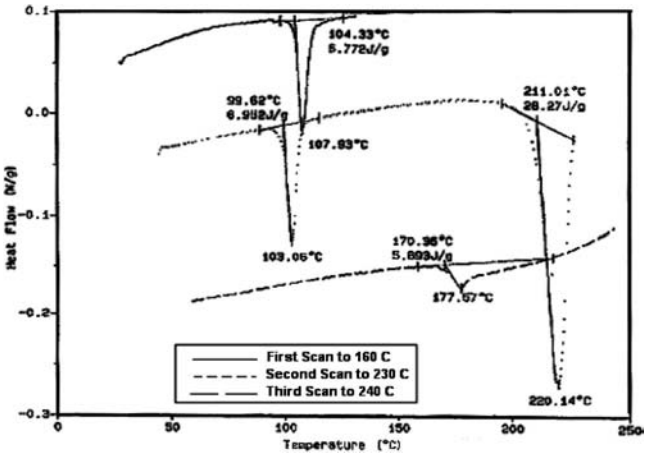

Figure 4. **Repetitive DSC scans of anhydrous Form I (sample 46).**

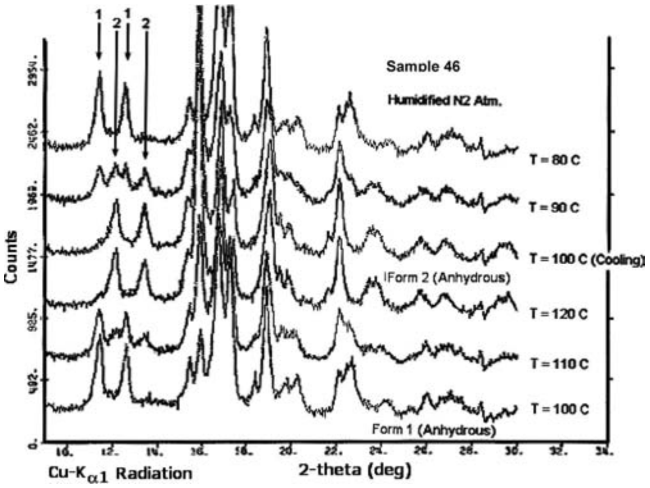

Figure 5. **XRPD of Form II dynamically reverting to anhydrous Form I (sample 46).**

Hygroscopicity studies performed at 52% and 100% relative humidity (RH) indicated that Form I formed a heptahydrate at typical laboratory temperatures and quickly became anhydrous above approximately 60–80 °C in a dry atmosphere. This conclusion was derived from TGA weight loss results shown in Figure 6. Evolved gas (EG) analyses using TG/MS were performed to confirm that only water evolved below approximately 100 °C (see Figure 6). Therefore, the observed weight losses can be used to determine the water content accurately. The water content found from samples stored in either 52% or 100% RH corresponds very closely to the theoretical 13.99% for a heptahydrate. Above approximately 120 °C, trace levels of acetone were observed from the TG/MS experiment. During and immediately following the melt, additional quantities of acetone, carbon dioxide, and other volatiles evolved, which indicates thermal degradation. Thermal degradation after the melt was also indicated by exothermic behavior observed from the DSC experiments and by visual observation of yellowing color with bubble formation in the melt. Additional evidence that Form I formed a heptahydrate is provided by XRPD results obtained under flowing nitrogen and switching between dry and 70% RH conditions. Upon

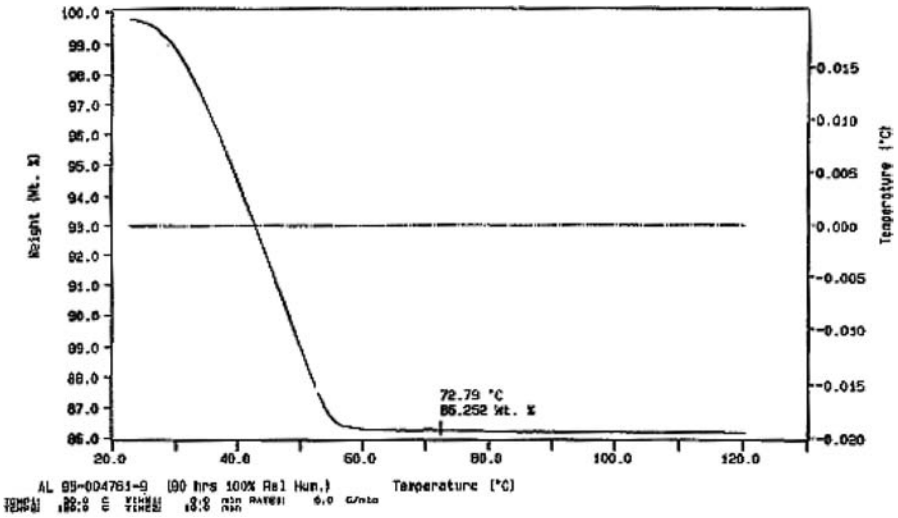

Figure 6. **TGA of Form I (sample 46) after storage at 100% RH for 90 h.**

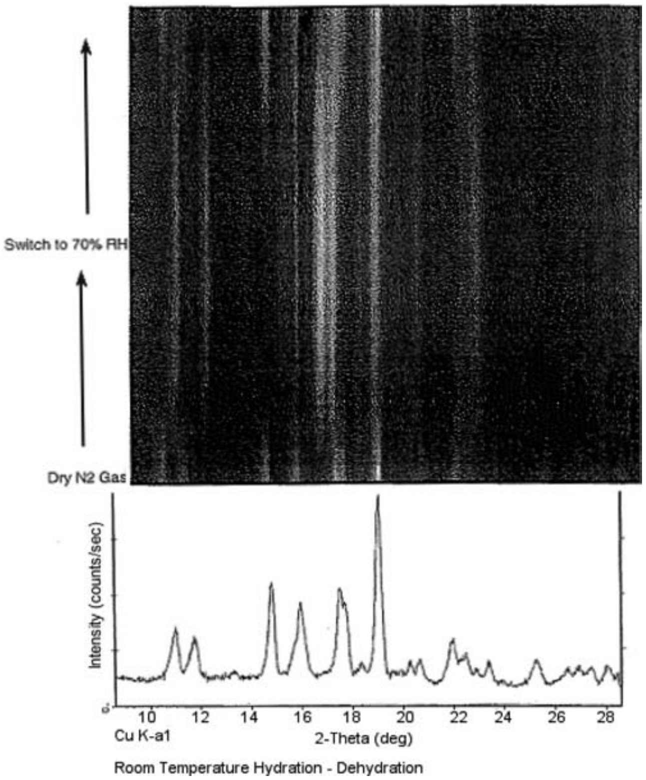

Figure 7. **XRPD of Form I (sample 46) swept with dry nitrogen and then with 70% RH nitrogen.**

changing from 70% to 0% RH, the XRPD pattern was observed to change from the heptahydrate Form I to the anhydrous Form I, Figure 7. Switching back to 70% RH reproduces the heptahydrate Form I XRD pattern. The XRPD and TGA results confirmed that Form I can be reversibly converted to a heptahydrate.

Room temperature XRPD results on several dehydrated Form I samples have been run. Although the XRPD data indicate that all of these samples are anhydrous Form I, the DSC results for samples 10 and 11 do not show a sharp solid–solid phase transition at 110 °C, which is typical of other Form I samples (see Figures 8 and 9). The lack of any additional peaks in the XRPD patterns would imply the presence of an amorphous material and/or an impurity. Note that both of these samples also have atypical preparations (see Table 1). Additional analyses would be needed to interpret the DSC results from these two samples. The DSC results for sample 9 were also atypical of Form I samples. Trace quantities of acetone were also observed in this region, but acetone did not contribute very

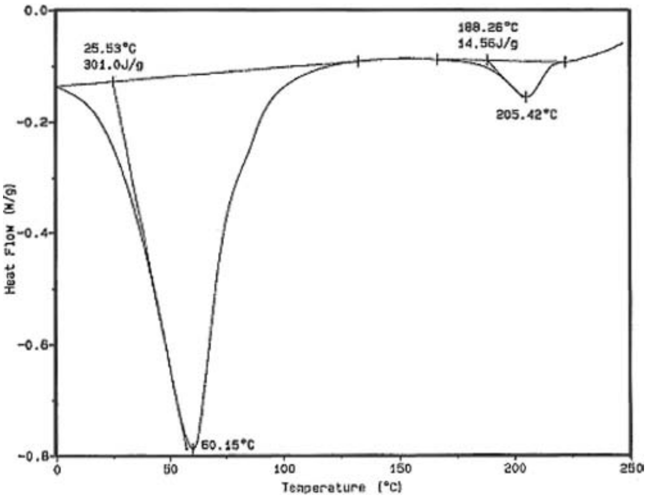

Figure 8. **DSC of atypical hydrated Form I (sample 10).**

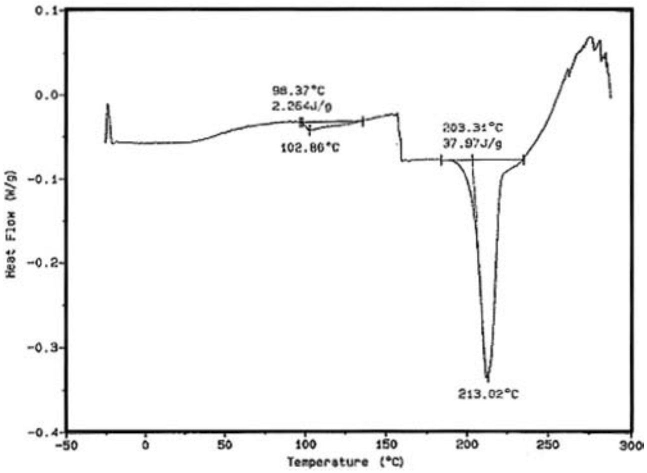

Figure 9. **DSC of atypical anhydrous Form I (sample 11).**

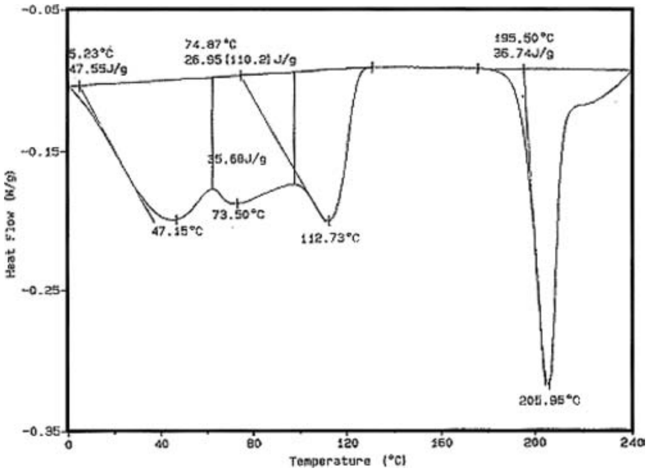

Figure 10. **DSC of hydrated Form III (sample 35).**

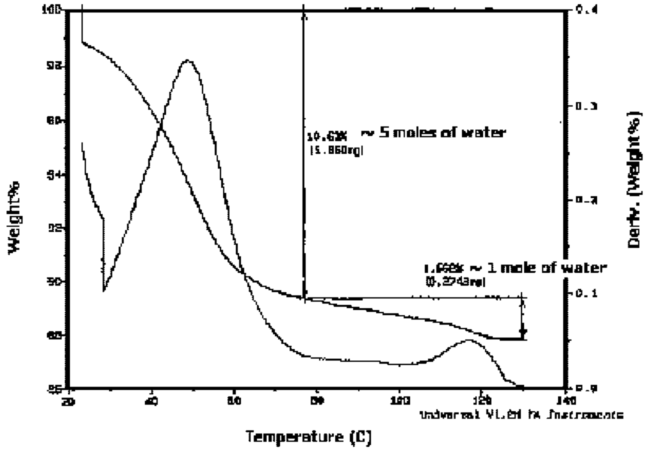

Figure 11. **TGA of hydrated Form III (sample 49).**

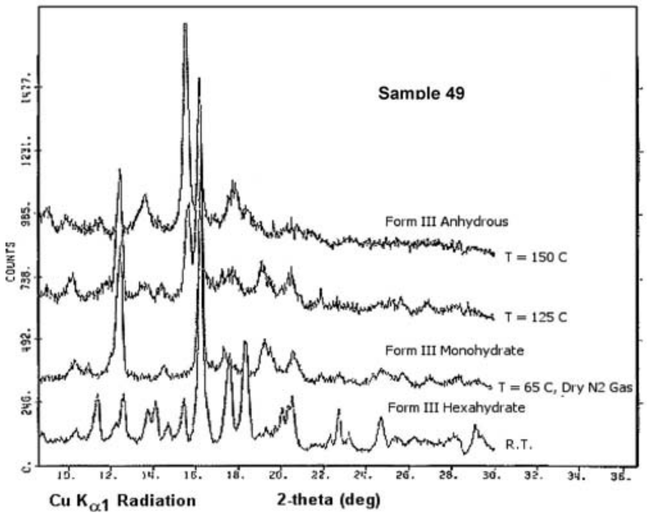

Figure 12. **XRPD of dynamic loss of water from Form III hexahydrate to make Form III monohydrate and then anhydrous Form III (sample 49).**

much to the 0.15% weight loss, as indicated by a poor correlation between the acetone evolution profile and the weight loss derivative. The heat observed from the broad endotherm was approximately 2.5 J/g and may be due to the heat of vaporization of water. Additional studies would be required to determine the source of water and carbon dioxide which were evolved.

Form III.

$$\text{I Disodium Salt in Water/Acetone} \xrightarrow{\text{Crash Precipitate}} \text{Form III x 6 } H_2O$$

$$\text{Form III x 6 } H_2O \xrightarrow[\text{in 82/18 acetone/water}]{\text{Digest > 10 h}} \text{Form I x 7 } H_2O$$

$$\text{Form III x 6 } H_2O \xrightarrow[T > 100\ ^{\circ}C]{}$$

$$\text{Form III x } H_2O \xrightarrow[T > 120\ ^{\circ}C]{} \text{Form III Anhydrous}$$

$$\text{Form III Anhydrous} \xrightarrow[\text{Water in atmosphere}]{} \text{Form III x 6 } H_2O$$

Form III has typically been produced during a 2 h purification re-slurry in 95/5 (v/v) acetone/water solution. The only apparent reproducible difference between the conditions that lead to Form III, instead of Form I, is that the slurry had been lightly refluxed at approximately 57 °C. In fact, Form I can be converted to Form III by refluxing a slurry in 95/5 acetone/water. Form III, however, cannot be converted back to Form I by slurrying the sample in 95/5 acetone/water at lower temperatures. Fairly subtle changes in the crystallization conditions can lead to the production of Form III.

Form III is uniquely identified in DSC analyses by the presence of a large endotherm below 100 °C due to water evolution, a smaller broad overlapping endotherm between 100 and 120 °C (also due to water loss), and a melt onset between 189 and 196 °C (with an apparent heat of fusion of 25–40 J/g). A representative DSC scan of Form III samples is shown in Figure 10. The relatively large variation in the heat of fusion is due to imprecise integration caused by baseline uncertainty and by the varying quantities of water in the samples. Corrections due to varying water content have not been made in these data.

Evolved gas (EG) analysis of sample 49 indicated that water was the only significant volatile observed during heating to 120 °C. Trace levels of carbon dioxide were also observed over this temperature region. Trace levels of acetone evolution were observed between 140 and 200 °C. Hygroscopicity studies, whereby sample 49 was stored at 52% RH for 18 h, indicated that Form III forms a hexahydrate. The TGA results are shown in Figure 11 and indicate that 5 mol of water evolve below approximately 100 °C, and the last mole of water evolves between 100 and 120 °C. XRPD data from DSC/XRPD analysis of sample 49, shown in Figure 12, confirm the formation of the intermediate hydrate and the conversion to anhydrous Form III above 125 °C. Additional XRPD experiments, performed by changing the nitrogen atmosphere between 0 and 70% RH at room temperature, show that the anhydrous Form III quickly converted back to a monohydrate at 70% RH (see Figure 13). To show that anhydrous Form III can be converted back to the hexahydrated Form, sample 49 was heated to 130 °C and subsequently stored at 52% RH at room temperature for 5 days. The sample was then analyzed by TGA and produced a 12.1% weight loss, with the same weight loss profile as the hexahydrate Form III. The TGA, EG, and DSC/XRD results show that Form III formed a hexahydrate during storage at 52% RH and that it

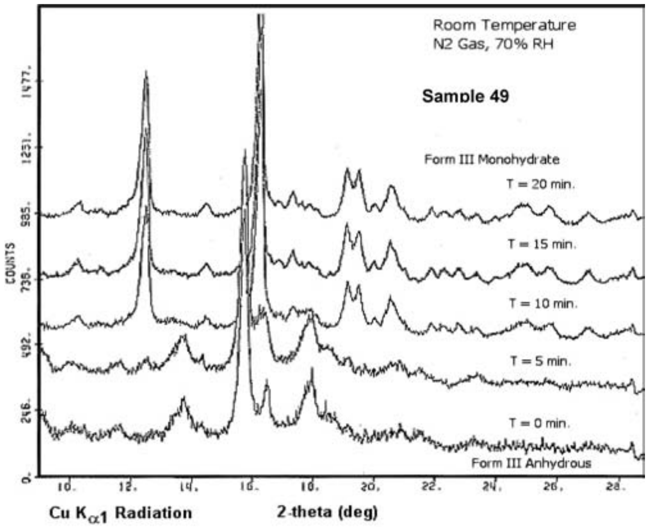

Figure 13. **XRPD of anhydrous Form III swept with 70 % RH nitrogen to make Form III monohydrate (sample 49).**

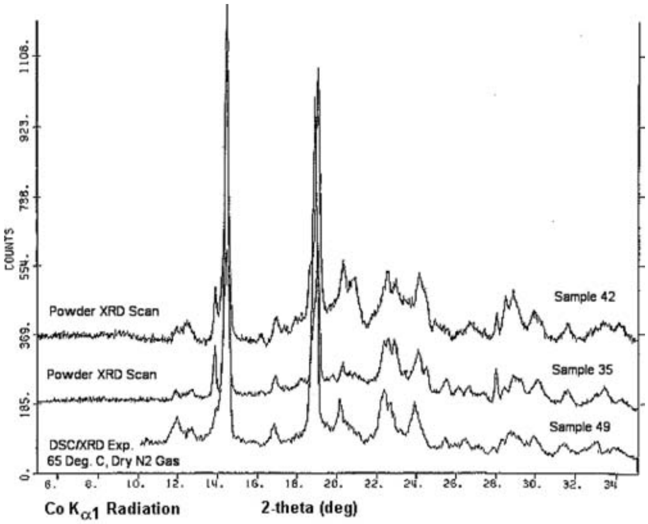

Figure 14. **Superimposed XRPD of three samples of Form III monohydrate (samples 42, 35 and 49, top to bottom).**

converted quickly to a monohydrate when heated to 100 °C. Above 125 °C, the anhydrous Form III is produced, which can be rehydrated to the hexahydrate.

A concern about the crystalline purity of the samples identified as Form III arose from the observation of an atypical sample of Form III, sample 42. The room temperature XRPD data from three different samples of the monohydrate Form III are shown in Figure 14. Sample 35 produced the typical DSC shown in Figure 10. The XRPD data for sample 49 was obtained during DSC/XRD experiments, wherein the monohydrate form was observed. Sample 49 also produced typical DSC results for Form III. Sample 42, however, produced an atypical DSC result, having an additional endotherm with an onset at approximately 223 °C and a peak at 236 °C (see Figure 15). This peak suggests the presence of another crystalline form. However, no significant differences are observed in the XRPD results. Sample 42 was produced from sample 35 by refluxing in acetone for 3.5 h (see Table 1). On closer examination of the typical DSC scans for Form III, a broad shoulder of varying size is often seen immediately following the melt. This could possibly represent a smaller manifestation of the larger peak observed in sample 42. This observation, combined with the XRPD results, suggests several possibilities, including that this new peak represents a thermally formed crystalline material, a minor quantity of another crystalline form, or an unstable polymorph which converted back to Form III between the DSC and XRPD experiments. Additional studies would be required to further understand the implications that sample 42 places on the assignment and DSC characterization of Form III.

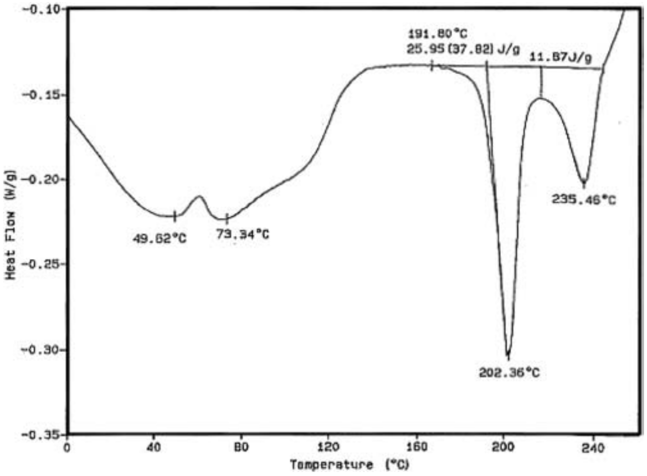

Figure 15. **DSC of atypical hydrated Form III (sample 42).**

Forms IV and V.

$$\text{Form III} \times 6\,H_2O \xrightarrow[\text{Heat in acetone}]{} \text{Form IV Hydrate}$$

$$\text{Form I} \times 7\,H_2O \xrightarrow[\text{Heat in 98/2 acetone/water}]{} \text{Form IV Hydrate}$$

$$\text{Form IV Hydrate} \xrightarrow[T > 80\,^{\circ}C]{}$$

$$\text{Form IV Anhydrous} \xrightarrow[T > 180\,^{\circ}C]{} \text{Form V}$$

Only two samples of pure Form IV have been produced and analyzed in this study. XRPD data for the two samples are shown in Figure 16. Sample 30 was produced from atypical conditions involving an extended reflux time (7+ h) of Step 1 material in 95/5 acetone/water. Sample 57 was produced from a Form I sample by refluxing for 2 h in 95/5 acetone/water. This was an operation that had typically produced Form III.

Form IV is identified in DSC analyses by the presence of two or three overlapping endotherms below 80 °C due to water evolution (see Figure 17). EG analysis performed on sample 57 confirmed that only water evolved below 80 °C and that trace quantities of acetone evolved between 120 and 190 °C (less than 0.1%). In sample 57, a second endotherm occurred, having an onset between 170 and 179 °C, due to a nonreversible solid–solid phase transition to the anhydrous Form V. A heat of approximately 10 J/g was observed. Form V subsequently melted with an onset of approximately 245 °C and a peak at approximately 256 °C. XRPD data from DSC/XRPD analysis are shown in Figure 18. This provides evidence of the solid–solid phase transition and the existence of a hydrous Form IV. At approximately 70 °C (not shown) the hydrous Form IV

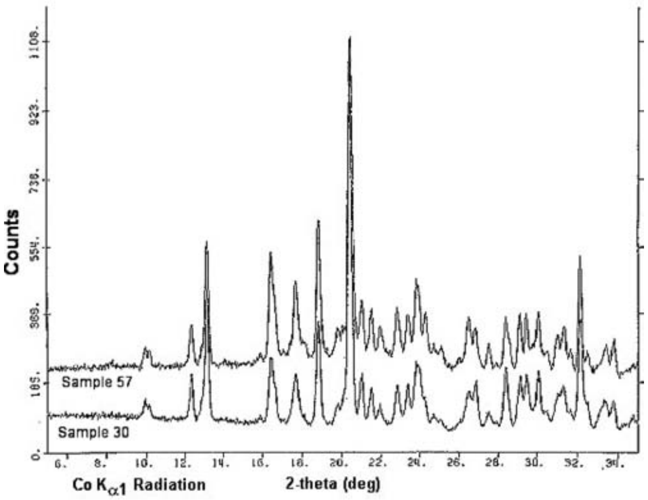

Figure 16. **XRPD of hydrated Form IV (samples 30 and 57).**

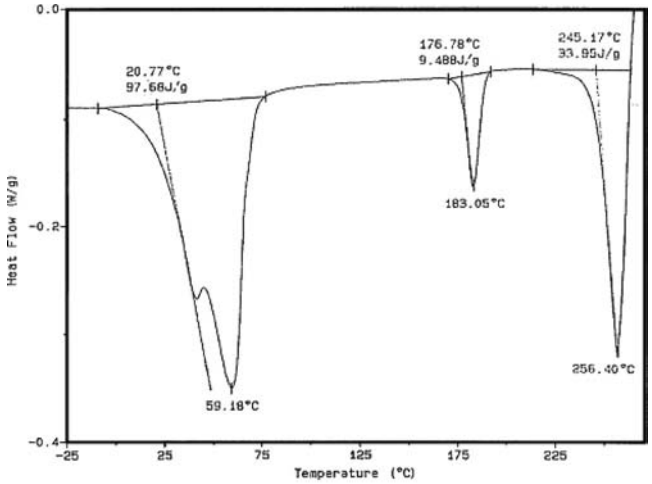

Figure 17. **DSC of hydrated Form IV (sample 57).**

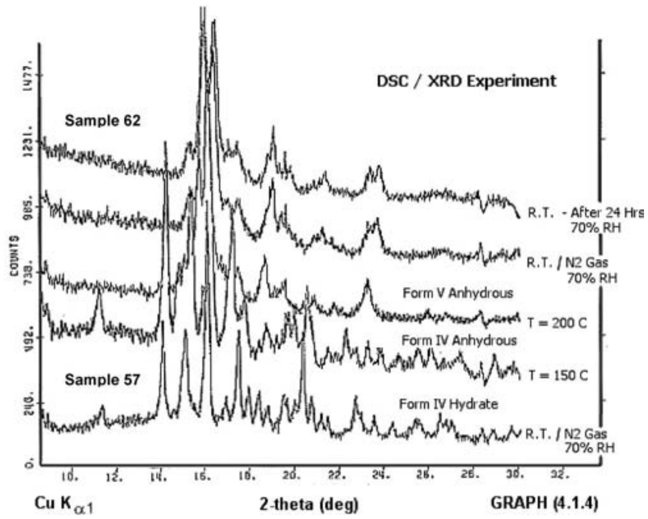

Figure 18. **XRPD of dynamic loss of water from Form IV hydrate to make anhydrous Form IV, then non-reversible transition to make anhydrous Form V (sample 57/62).**

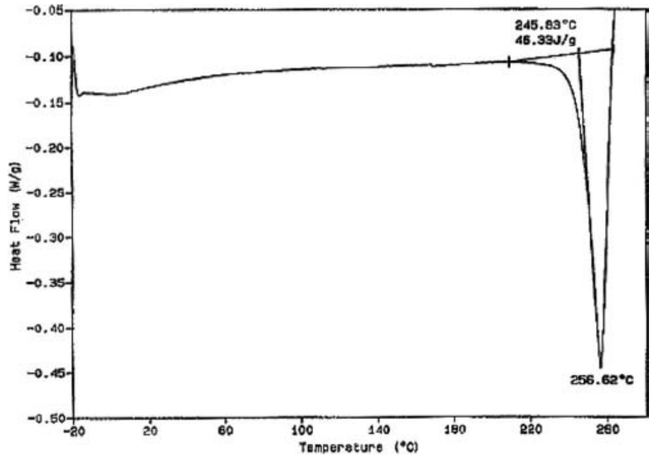

Figure 19. **DSC of anhydrous Form V (sample 62).**

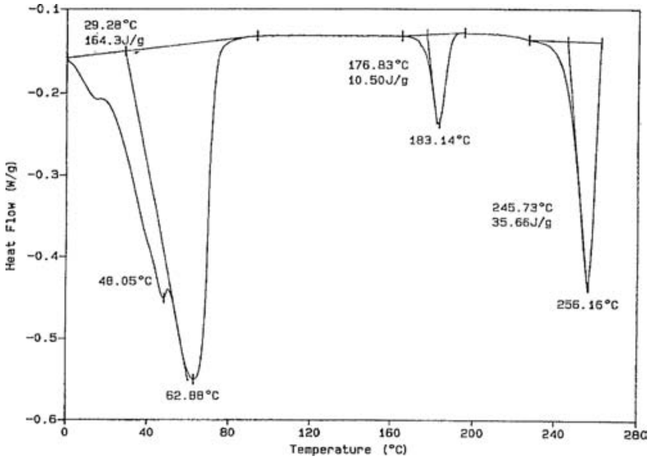

Figure 20. **DSC of Form IV hydrate (sample 57) after storage at 52% RH for 42 h.**

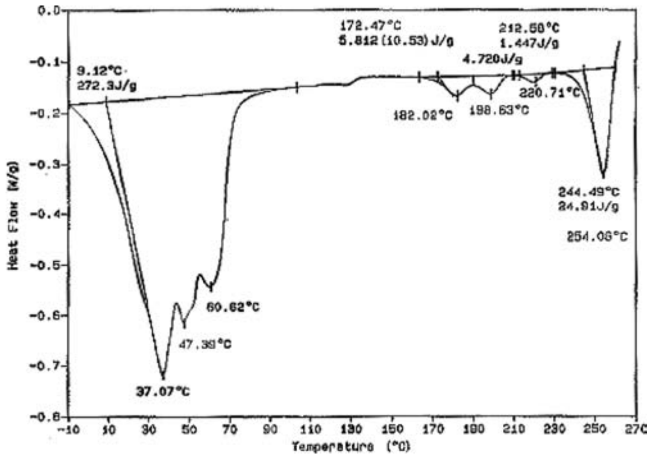

Figure 21. **DSC of Form IV hydrate (sample 57) after storage at 90% RH for 20 h; partial conversion to hydrated Forms I and III.**

was observed to convert to the anhydrous Form IV, as evidenced by changes in the XRPD pattern. At about 180 °C, the powder diffraction pattern began to change again, indicating the structural conversion to anhydrous Form V. As the sample was cooled to room temperature, the XRPD pattern did not change, showing that anhydrous Form V structure was stable over the time scale of the experiment. The nonreversible character of the solid–solid phase transition was also indicated by a DSC scan of sample 62, which was the anhydrous Form V from sample 57 previously heated to 200 °C in an anaerobic

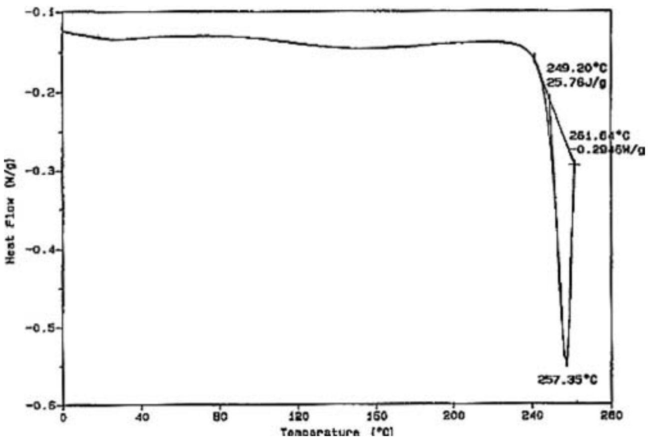

Figure 22. **DSC of anhydrous Form VI (sample 40).**

atmosphere (see Figures 18 and 19>). Finally, HPLC analysis was performed on a portion of sample 57, after it had been thermally converted to Form V (sample 62). The HPLC results yielded a retention time consistent with **1** disodium salt and a peak area indicating a purity of 96.2%. This result largely rules out the possibility of a chemical modification occurring at 180 °C. The hygroscopic nature of Form IV was investigated by studying sample 57 under 52% and 90% RH conditions. DSC results are shown in Figures 20 (for RH 52%) and 21 (for RH 92%). Very little change was observed in the DSC after storage of the sample at 52% RH for 42 h. Storage at 92% RH, however, resulted in drastic changes in the DSC pattern. Evidence of other crystalline forms is demonstrated by small endotherms peaking at approximately 199 and 221 °C. A small endotherm at approximately 120 °C, which overlaps with the much larger water loss endotherm below 80 °C, was also observed. These results suggest that Form IV has partially converted to Form I and Form III during the 20 h at 92% RH. TGA results obtained from the sample after storage at 52% RH indicate a 7.9% water loss. This corresponds to approximately 3.8 mol of water. The reversible conversion between hydrous and anhydrous Form IV was demonstrated by a room temperature XRPD experiment in which the atmosphere was alternated between 0 and 70% RH. Form IV was found to convert between the hydrous and anhydrous forms within 15 min at room temperature.

The anhydrous nature of Form V was studied using XRPD. The room temperature XRPD pattern of Form V, which was created from sample 57 by heating to 200 °C in anaerobic conditions during a DSC/XRD experiment, is shown in Figure 18. After cooling, the Form V sample was kept under a flowing 70% RH nitrogen atmosphere for 24 h, but the XRPD pattern did not change. This confirmed that Form V remained anhydrous under these conditions. Thermal degradation occurred rapidly during and immediately following the melt of Form V. The sample was observed to bubble and turn yellow as it melted. This observation suggests that the apparent heat of fusion as determined by DSC will be highly variable. In addition, thermal

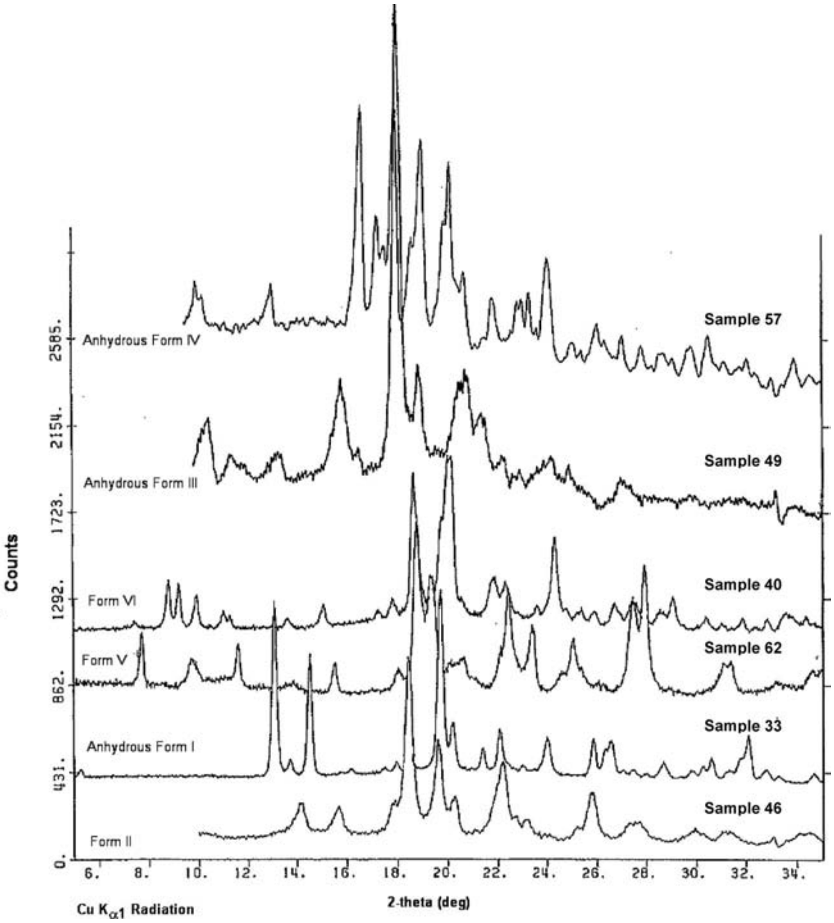

Figure 23. **Superimposed XRPD of anhydrous Forms II, I, V, VI, III, and IV (samples 46, 33, 62, 40, 49, and 57, respectively, bottom to top).**

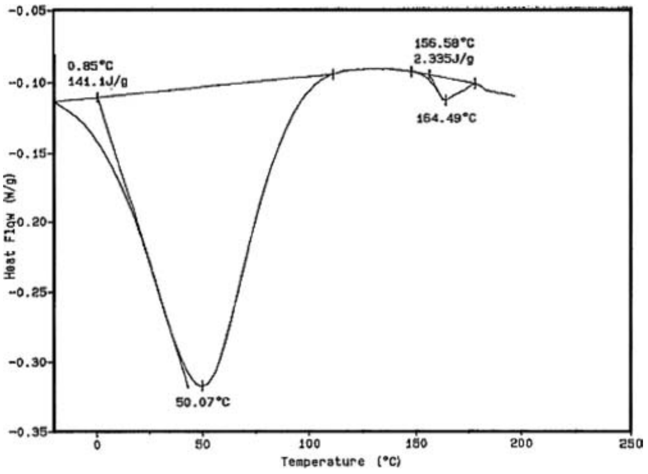

Figure 24. **DSC of amorphous Form (sample 26)**

degradation may begin prior to the sample melt, causing a depression of the observed melt temperature. This could result in large variations of the observed melt onset and peak temperatures, which would be affected by sample surface area, DSC scanning speed, and the sample thermal conductivity.

Form VI.

Form I (hydrate/anhydrous) $\xrightarrow[\text{Heat in dry acetone}]{\hspace{4em}}$ Form VI

Form III or IV $\xrightarrow[\text{Heat in dry acetone}]{\hspace{4em}}$ Form VI

Form III or VI $\xrightarrow[\text{82/18 acetone/water at 20 °C}]{\hspace{4em}}$ Form I x 7 H_2O

A single sample of Form VI was produced during a purification re-slurry in refluxing 100% acetone. The DSC results for sample 40 are shown in Figure 22. This sample was not dried prior to receipt and did not show any evidence of water loss as indicated by the lack of endothermic activity prior to the melt. Form VI has been shown to remain anhydrous even under 100% RH conditions at room temperature. A melt onset is observed at approximately 249 °C. Unfortunately, this melt temperature does not allow differentiation between Form VI and Form V. Fortunately, XRPD analysis does provide differentiation of Form VI from all of the other crystalline forms characterized in this study. To illustrate this point, the XRPD patterns for each known anhydrous form are shown in Figure 23 for direct comparison.

Amorphous Form. The **1** disodium salt can be lyophilized from water solution to produce another solid form. This form was analyzed and found to be amorphous by DSC and XRPD. The DSC scans (Figure 24) show a large broad single endothermic peak observed below 100 °C, plus a small endothermic peak with an onset between 149 and 161 °C and a heat of approximately 2 J/g. EG analysis performed on sample 26 confirmed that the large endotherms below 100 °C were due to water evolution. An XRPD pattern for amorphous sample 26 is given in Figure 25. A TGA study indicated that sample 26 lost 4.4% weight due to water evolution below 100 °C. The small endotherms observed at about 150 °C corresponded with the evolution of approximately 0.1% acetic acid. The endotherms are not, however, primarily due to the vaporization of acetic acid from the amorphous sample. This conclusion is based on multiple DSC re-scans of sample 26, wherein the transition is repeatedly observed. The endotherm may represent a glass transition combined with the onset of thermal degradation, or the melt of a minor quantity of crystalline material that recrystallized upon cooling from the melt.

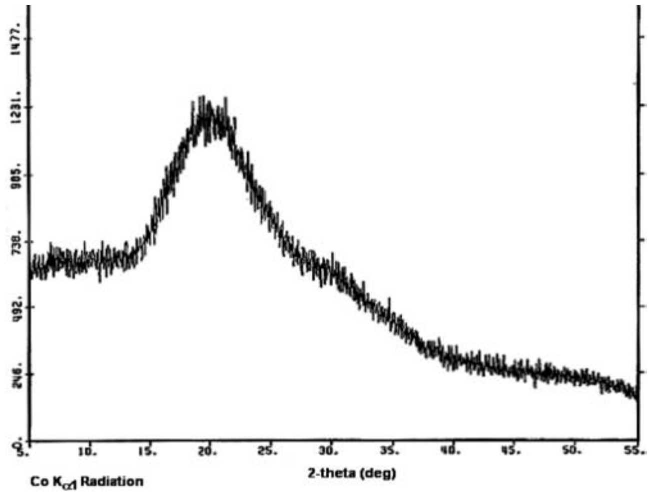

Figure 25. **XRPD of amorphous Form (sample 26)**

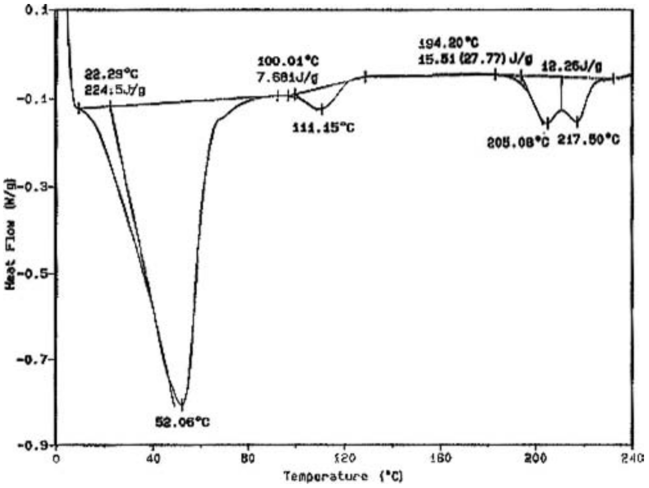

Figure 26. **DSC of mixture of hydrated Forms I and III (sample 45).**

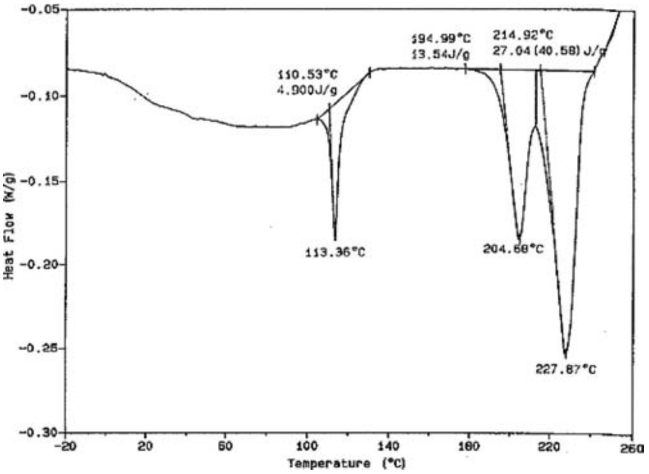

Figure 27. **DSC of mixture of anhydrous Forms I and III (sample 60).**

Scheme 1. **Interconversions of polymorphs of 1 dicarboxylate disodium salt**

$$\text{Form I} \times 7\,H_2O \xrightleftharpoons[\text{Water in atmosphere}]{T > 80\ ^\circ C} \text{Form I anhydrous} \xrightleftharpoons[T < 110\ ^\circ C]{T > 110\ ^\circ C} \text{Form II}$$

$$\text{I Disodium Salt in Water/Acetone} \xrightarrow{\text{Crash Precipitate}} \text{Form III} \times 6\,H_2O$$

$$\text{Form III} \times 6\,H_2O \xrightarrow[\text{in 82/18 acetone/water}]{\text{Digest > 10 h}} \text{Form I} \times 7\,H_2O$$

$$\text{Form III} \times 6\,H_2O \xrightarrow[T > 100\ ^\circ C]{} \text{Form III} \times H_2O \xrightarrow[T > 120\ ^\circ C]{} \text{Form III Anhydrous}$$

$$\text{Form III Anhydrous} \xrightarrow[\text{Water in atmosphere}]{} \text{Form III} \times 6\,H_2O$$

$$\text{Form III} \times 6\,H_2O \xrightarrow[\text{Heat in acetone}]{} \text{Form IV Hydrate}$$

$$\text{Form I} \times 7\,H_2O \xrightarrow[\text{Heat in 98/2 acetone/water}]{} \text{Form IV Hydrate}$$

$$\text{Form IV Hydrate} \xrightarrow[T > 80\ ^\circ C]{} \text{Form IV Anhydrous} \xrightarrow[T > 180\ ^\circ C]{} \text{Form V}$$

$$\text{Form I (hydrate/anhydrous)} \xrightarrow[\text{Heat in dry acetone}]{} \text{Form VI}$$

$$\text{Form III or IV} \xrightarrow[\text{Heat in dry acetone}]{} \text{Form VI}$$

$$\text{Form III or VI} \xrightarrow[\text{82/18 acetone/water at 20 } ^\circ C]{} \text{Form I} \times 7\,H_2O$$

Mixtures of Forms. Using the DSC and XRPD profiles discussed above for the several pure polymorphic forms of this study, we were able to assign combinations of two or more polymorphs as contributing to several samples which were isolated. These results are summarized in Table 4. In many cases the mixture of polymorphs can be accounted for by the addition of the DSC results of the component pure polymorphs. In some cases, however, the assignment of component polymorphs to sample mixtures depended on the XRPD results.

3. Conclusions

Interconversions of the Polymorphs of 1 Disodium Salt. The interconversions of polymorphs of the **1** disodium salt have been studied extensively in this research program. The experimental conditions required for these interconversions are fairly well understood, but more research needs to be done to more fully understand the relationships among the polymorphs. Heats of solution of the various polymorphs need to be measured, in order to prove the relative order of stabilities for these solid forms. At the present we suspect that polymorph Form I is the most stable form, since we are able to convert Forms III, IV, and VI to Form I by digestions over a period of hours to days. However, Form VI has been observed only in the anhydrous state. The anhydrous nature of Form VI may make this polymorph the most ideal crystalline material for subsequent formulation. At present we know little about a potential new polymorph, Form VII. Form VII was apparently formed by refluxing a mixture of Form I and Form IV or by refluxing Form VI in acetone. The proposed interconversions of the various polymorphs of **1** dicarboxylate disodium salt are given in Scheme 1.

Detection of Mixtures of Polymorphs and Potential New Solids Forms. By using the combined and dynamic DSC/XRPD, several mixtures of **1** disodium salt samples were identified, and the components of these mixtures were assigned. Reversible and irreversible structural transformations between different hydrated and anhydrous polymorphs were documented as well. In a few cases some potential new solid forms were suggested, as part of these mixtures. Kinetics of the transformations between solid forms and between hydrated versus anhydrous versions of a given form (at varying humidity levels) can be run using the DSC/XRPD instrument. These rate determinations were not done in the present study.

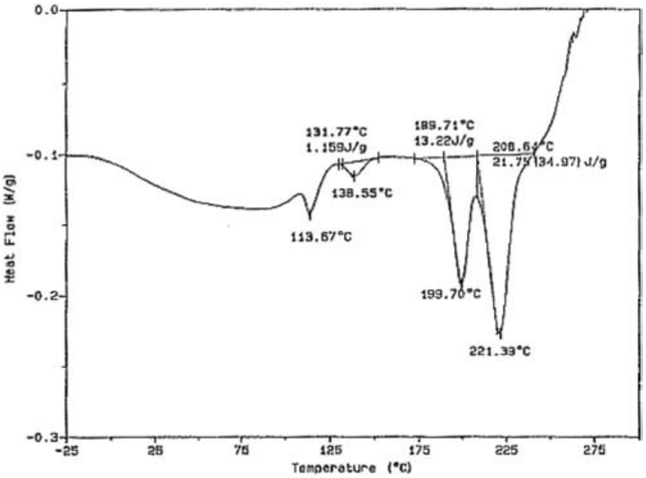

Figure 28. **DSC of mixture of anhydrous Form I and monohydrate Form III (sample 58).**

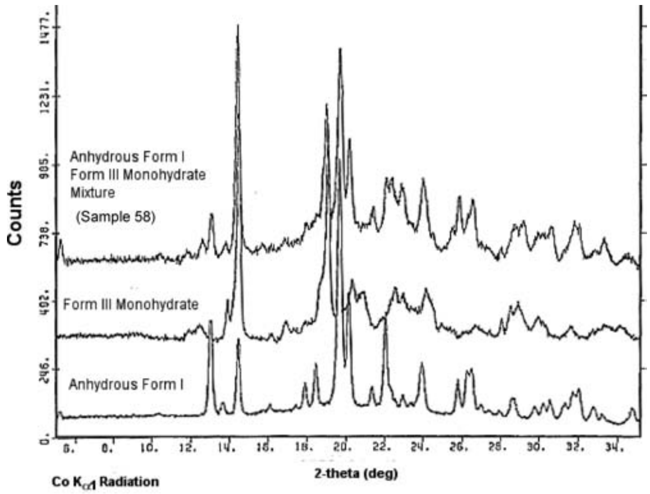

Figure 29. **XRPD of mixture of anhydrous Form I and monohydrate Form III (sample 58).**

4. Experimental Section

DSC Conditions. DSC analyses were performed using a TA 2910 DSC with open aluminum pans (TA Instruments; no. 900793.901 or 990999.901). The samples were heated using a scan rate of 5 °C/min with a 30 mL/min prepurified nitrogen purge.

Evolved Gas Analysis. Simultaneous TG/MS and TG/gas chromatography (GC)/MS analysis were performed on several samples. A split was used to send a fraction of the evolved gases to a quadruple mass spectrometer for real time detection of the volatiles over the duration of the thermogravimetric analysis. Simultaneously, a second split was also used to direct another small fraction of the evolved gases to a cryotrap (at approximately −180 °C) during the entire experiment. After the thermogravimetric program was complete, the trapped volatiles were analyzed using sub-ambient GC/MS.

TGA Conditions. TGA analysis was performed on several samples using a TA 2950 TGA with a platinum pan. A nitrogen atmosphere was used for each trial. Some analyses were performed on a Perkin Elmer-7 TGA with an aluminum pan. A nitrogen atmosphere was also used for these trials.

XRPD Conditions. X-ray powder diffraction patterns were collected for several samples as received or after storage over anhydrous calcium sulfate. The samples were mounted in zero scatter sample holders for analysis. The XRPD patterns were collected using a Siemens D-500 automated powder diffractometer equipped with a Co X-ray tube source, primary beam monochromator, and a position sensitive detector (PSD). The incident beam was collimated using a 1° divergent slit. The active area on the PSD subtended approximately 5° 2θ. The source was operated at 35 kV and 30 mA, and the samples were illuminated with Co $K\alpha_1$ radiation, $\lambda(K\alpha_1) = 1.788965$ Å. XRPD data were collected from 5° to 55° 2θ at a rate of 0.5° 2θ/min with a step width of 0.02° 2θ. Samples were rotated throughout data collection, to maximize sampling statistics.

DSC/XRPD Conditions. Simultaneous DSC/XRPD data were collected for several samples 46 (see Table 3). The DSC/XRPD experiments were performed in an inert atmosphere under either dry or humidified (70% RH) conditions. The DSC/XRPD instrument (shown in Figure 1) was a Dow-developed technology,[24,25] which utilized a copper X-ray source and germanium monochromator to produce copper $K\alpha_1$ radiation at a wavelength of 1.540600 Å. The X-ray data was collected using an MBraun curved PSD with a chamber depth of 1 cm. The focal radius of the system was 57 mm, and the 5 cm length of the PSD subtended ~25° 2θ of the diffraction pattern. The DSC component was a second generation custom-built calorimetry cell, which had a temperature range of −45 to 600 °C, with temperature accuracy of ±0.1 °C, equivalent to commercial calorimeters available in the mid-1990s. Both the DSC and XRPD programming and data collection were under computer control. A digital hygrometer (Fisher Scientific model 11-661-7A) was placed near the sample position in the DSC/XRPD instrument to determine the relative humidity (RH) at room temperature. The experimental parameters for the DSC/XRPD studies are described in Table 5.

Hygroscopicity Studies. Four different humidity environments were prepared to produce 0, 52%, 92%, and 100% RH. Zero RH was accomplished by storing the samples over calcium sulfate desiccant. The 52% and 93% RH conditions were produced by storage of samples in a container in equilibrium with saturated aqueous solutions of sodium sulfate and magnesium nitrate. The 100% RH condition was achieved by placing the sample in a closed container in equilibrium with pure water. The temperature varied with the laboratory temperature (typically between 23 and 26 °C).

Table 5. **Experimental parameters for typical DSC/XRD studies**

study		temperature program			
polymorph	purge gas/flow rate	start (°C)	end (°C)	rate (°C/min)	hold (min)
dry-heat (I)	dry N_2 gas, 100 cc/min	25	125	1	10
dry-cool (I)		125	25	–1	
wet-heat (I)	humidified N_2 gas, 100 cc/min	25	125	1	10
wet-cool (I)		125	25	–1	
dry-heat (III)	dry N_2 gas, 100 cc/min	25	150	5	10
dry-cool (III)		150	30	–2	
wet-heat (III)	humidified N_2 gas, 100 cc/min	25	150	2	10
wet-cool (III)		150	30	–2	
wet-heat (V)	humidified N_2 gas, 100 cc/min	30	75	1	1
wet-heat (V)		75	155	10	0
wet-heat (V)		155	185	1	0
wet-heat (V)		185	200	10	5
wet-cool (V)		200	100	–10	0
wet-cool (V)		100	30	–2	0

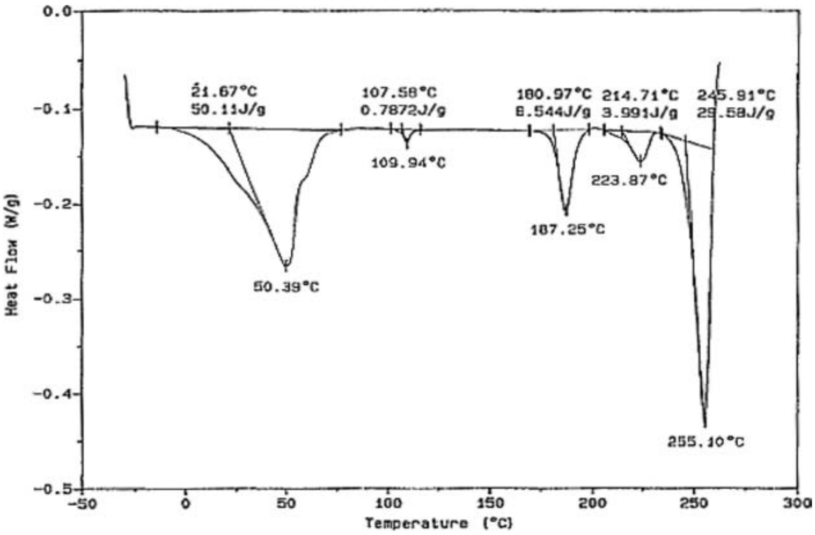

Figure 30. **DSC of mixture of hydrated Forms I and IV (sample 8).**

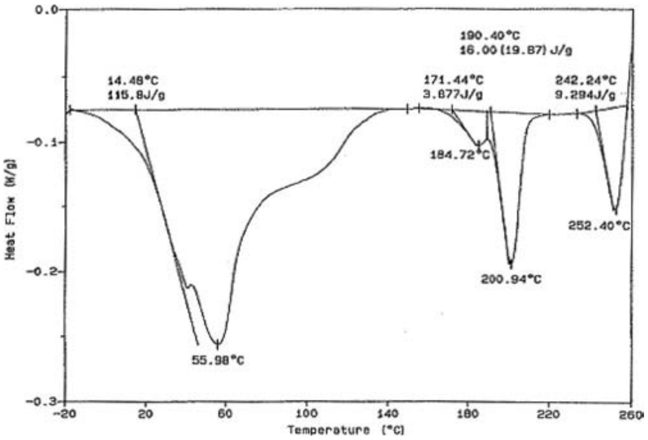

Figure 31. **DSC of mixture of Form III monohydrate and Form IV hydrate (sample 56).**

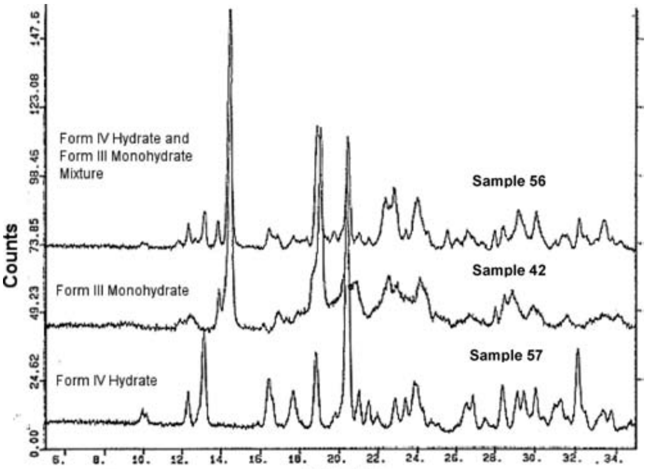

Figure 32. **Superimposed XRPD of mixture of Form III monohydrate and Form IV hydrate (sample 56) versus authentic Form III monohydrate (sample 42) and authentic Form IV hydrate (sample 57).**

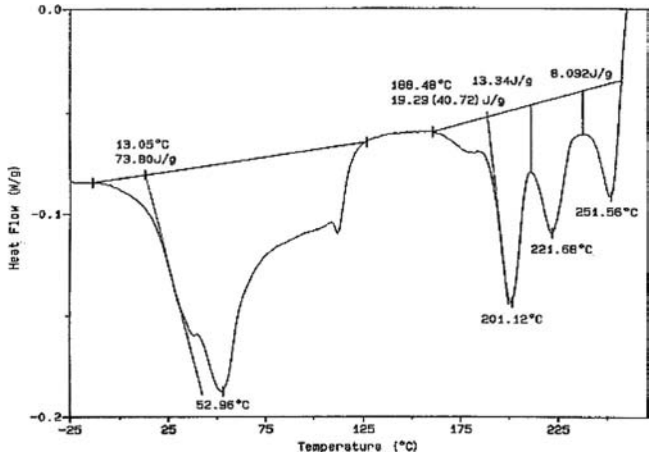

Figure 33. **DSC of mixture of hydrates of Forms I, III, and IV (and possibly VI) (sample 59).**

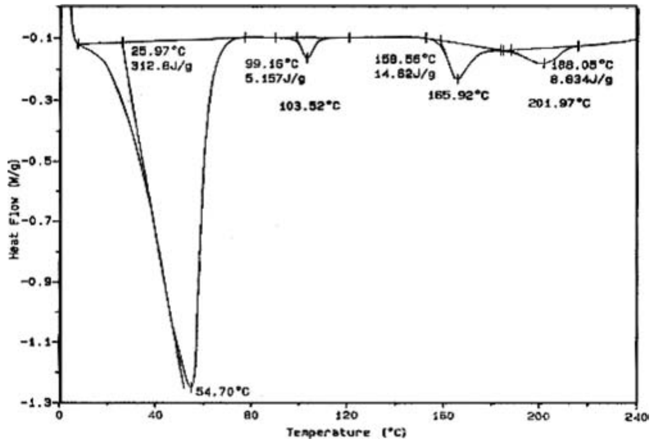

Figure 34. **DSC of mixture of hydrated Form I and possible unknown new form (sample 52).**

Conversion of 1 Dicarboxylic Acid to 1 Dicarboxylate Disodium Salt Form I. The **1** dicarboxylic acid (42.00 g) was loaded into a reactor, along with sodium bicarbonate (9.80 g, 116.6 mmol), 105 mL of water (deionized), and 105 mL of acetone. The mixture was heated with stirring to 45 °C, at which temperature all solids dissolved, to form a clear, colorless solution. To the solution was slowly added 140 mL of acetone. The resulting solution was cooled slowly, and solids began forming at a solution temperature of 43 °C. The resulting slurry

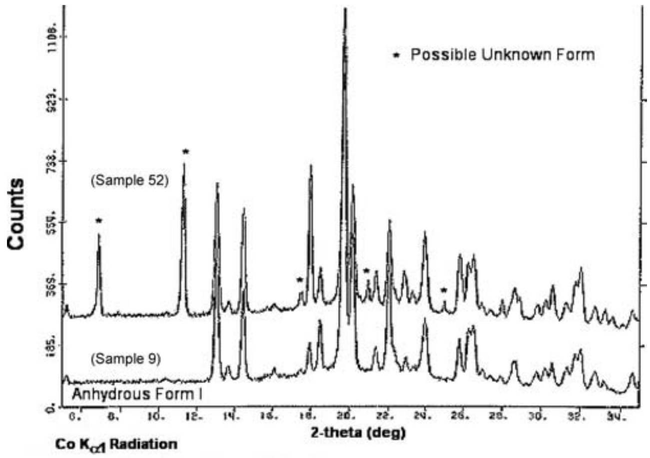

Figure 35. **XRPD at high temperature of mixture of anhydrous Form I and possible unknown new form (sample 52) versus XRPD of anhydrous Form I (sample 9).**

cooled from 43 to 39 °C over a 50 min period (to become a thick slurry) and from 39 to 31 °C over a 60 min period. The slurry was cooled from 31 to 11 °C over a 25 min period. The solids were collected by filtration, and the filtercake was washed with 60 mL of acetone at ambient temperature. The wetcake was dried under vacuum at 51 °C overnight, to obtain 37.9 g of **1** dicarboxylate disodium salt as Form I hydrate. The above procedure is "Step 1".

Direct Conversion of 1 Diacid to Form III of 1 Diacid Disodium Salt. The **1** dicarboxylic acid (10.00 g) was added to a reactor, followed by sodium bicarbonate (2.33 g), 25 mL of deionized water, and 25 mL of acetone. The stirred mixture was heated to 53 °C, to obtain a clear solution. Additional acetone (89 mL) was added over a 15 min period, to obtain a clear solution at 49 °C (final solvent 82/18 (v/v) acetone/water). The solution was allowed to cool fairly quickly; after 15 min (47 °C) solids began forming. After 20 min (at 44 °C) a thick slurry had formed. The gel-like slurry was allowed to cool from 44 to 28 °C over a 55 min period. Note: this crash-cooling procedure was done so as to make **1** disodium salt Form III during the crystallization.

Conversion of Form III to Form I Hydrate of 1 Diacid Disodium Salt. The slurry of Form III was allowed to stand at ambient temperature overnight. After standing at ambient temperature for 14 h, the slurry was stirred for 8 h, during which time the slurry changed consistency from very thick to thin and could be easily stirred. The solids were collected by suction filtration. The filtercake was washed with 22 mL of acetone. The filtercake was dried under vacuum at 48 °C overnight, to obtain 8.8 g of white solids. The preparation of Form I hydrate from Form III involved either stirring the Step 1 wetcake in 95/5 (v/v) acetone/water at ambient temperature for more than 10 h or heating the Step 1 wetcake in 95/5 acetone/water below the reflux temperature for more than 1.5 h.

Conversion of Polymorph Mixtures of 1 Disodium Salt to Polymorph I by Heating in 95/5 (v/v) Acetone/Water. The entire wetcake of **1** disodium salt (prepared from 0.20 mol of **1** diacid by the Step 1 solution process) was loaded into a 2-L, three-necked, round-bottomed flask, which was fitted with an overhead stirrer and reflux condenser. To this flask was also added 1300 mL of an acetone/water (95/5 (v/v)) solution. The resulting stirred slurry was heated within a temperature range of 48–53 °C (maximum temperature, i.e., no reflux) for 2.7 h. The slurry was easily stirred through the digestion process. The slurry was cooled from 48 to 45 °C in 22 min, from 45 to 36 °C in 46 min, and from 36 to 18 °C in 20 min. The solids were collected by filtration at ambient temperature, and the filtercake was washed with 450 mL of ambient temperature acetone. The wetcake (weight 183 g) was dried overnight under vacuum at 69 °C, to obtain 139 g of Form I (91 % yield, based on original **1** diacid). The above procedure is "Step 2".

Conversion of Form I Hydrate to Form III of 1 Diacid Disodium Salt Sample 35. Form I heptahydrate (91 g) was heated with 900 mL of 95/5 (v/v) acetone/water. The slurry was heated to reflux for 1.1 h, during which time the slurry "set up" to form a "milkshake" consistency. The slurry was allowed to cool to 33 °C in 2 h. The slurry was cooled rapidly to 16 °C, and the solids were collected by filtration. The filtercake was washed with 300 mL of acetone. The wetcake (weight 123 g) was dried in a vacuum oven at 42 °C for 4 h, to obtain a final weight of 89 g. Further drying of 10.00 g of this material at 110 °C in a vacuum-pumped oven, resulted in a 6.30 % loss-on-drying.

Conversion of Polymorph Mixtures of 1 Disodium Salt to Form VI by Reflux in Acetone. Into a 1-L, three-necked, round-bottomed flask, fitted with an overhead stirrer and a reflux condenser, were put **1** disodium salt (25.00 g, as mixture of Form I and Form III) and 300 g of acetone. The resulting slurry was heated to reflux for 23 h. The stirred slurry was allowed to cool to ambient temperature. The solids were collected by suction filtration, and the solids were washed with 100 mL of fresh acetone. The solids were dried in a vacuum oven at 60 °C for 2.5 h, to obtain a final weight of 23.50 g of solids.

Received for review February 13, 2007.

OP700037W